

Locating Blood vessel in Retinal Images by Piecewise Threshold Probing of a Matched Filter Response

Dhanashri Dilip Dere¹, Dr.V.N.Nitnaware²

^{1,2} Student of Dept. of ENTC Engineering, jaihind college of engineering Kuran, Junnar, Pune

Abstract — we describe an automated method to locate and outline blood vessels in images of the ocular fundus. Such a tool should prove useful to eye care specialist for purpose of patient screening, treatment evaluation, and clinical study. Our method differs from previously known methods in that it use local and global vessel feature cooperatively to segment the vessel network. We evaluate our method using hand labeled ground truth segmentations of 20 images. A plot of the operating characteristic shows that our method reduces false positives by as much as 15 times over basic thresholding of a matched filter response (MFR), at up to a 75% true positive rate. For a baseline, we also compared the ground truth against a second hand – labeling, yielding a 90% true positive and a 4% false positive detection rate, on average. These numbers suggest there is still room for a 15% true positive rate improvement, with the same false positive rate, over our method. We are making all our images and hand labeling publicly available for interested researchers to use in evaluating related methods.

Keywords : Adaptive thresholding, blood vessel segmentation, matched filter, retinal imaging.

I. INTRODUCTION

Blood vessel appearance is an important indicator for many diagnoses, including diabetes, hypertension, and arteriosclerosis. Veins and arteries have many observable features, including diameter, color, tortuosity (relative curvature), and opacity (reflectivity). Artery - vein crossing and patterns of small vessels can also serve as diagnostic indicators. An accurate delineation of the boundaries of blood vessels makes precise measurement of these feature possible. These measurements may then be applied to a variety of tasks, including diagnosis, treatment evaluation, and clinical study. We describe an automated method to locate and outline blood vessels in images of the ocular fundus. With this tool eye care specialists can potentially screen larger populations for vessel abnormalities. Precise measurement may be more easily recorded, for instance, for evaluation of treatment or for clinical study (such as reported in [2]). observations based upon such a tool would also be more systematically reproducible.

previous method to segment blood vessel automatically have concentrated primarily on their local attributes. vessels may be characterized by the expected color (reddish), shape(curvilinear),gradient(strength of boundary), and contrast (with background). Unfortunately, this description is not exclusive. For suitable ranges of these attributes. Other image manifestations, such as the boundaries of the optic nerve and some hemorrhages and lesions, can exhibit the same local attributes as vessels.

Fig.1 shows the result of the matched filter convolution described in [3]. The strength of the matched filter response (MFR) is coded in grey scale :the darker a pixel, the stronger the response. Notice that the strong responses I the center of the MFR image, which are obviously not vessel, are unfortunately much stronger than the response of left side of the MFR image, which are vessel. Therefore, applying a single global threshold does not provide adequate classification, as shown in fig.2. a bilevel threshold (such as hysteresis) is also inadequate, because the vessel and nonvessel pixels with strong MFR's are usually specially connected, as in fig.1.

We propose a novel method to segment blood vessels that compliments local vessel attributes with region-based attributes of the network structure. A piece of the blood vessel network is hypothesized by probing an area of the MFR image, iteratively decreasing the threshold. At each iteration, region-based attributes of the piece are tested to consider probe continuation, and ultimately to decide if the piece is vessel. Pixels from probes that are not classified as vessel are recycled for further probing. The strength of this approach is that individual pixel labels are decided using local and region-based properties

II. RELATED WORK

1. X. Chen and A. L. Yuille, "Detecting and reading text in natural scenes," in *Proc. Comput. Vision Pattern Recognit.*, 2004, vol. 2, pp. II-366–II-373.

Previous method to segment blood vessels generally fall into three categories : window based [3],[16][17],[19], classifier based [5],[21], and tracking- based [20]-[23]. Window based methods, such as edge detection, estimate a match at each pixel for a given model against the pixel's surrounding window. In [3], the cross section of a vessel in a retinal

image was modeled by a Gaussian shaped curve and then detected using rotated matched filters. In [17], a similar method was used for artery detection in angiograms. In [19], a standard gradient filter was



Fig. 1. (a) An example retinal image with obscured vessels. (b) MFR. The response is coded such that a darker value represents a stronger response.

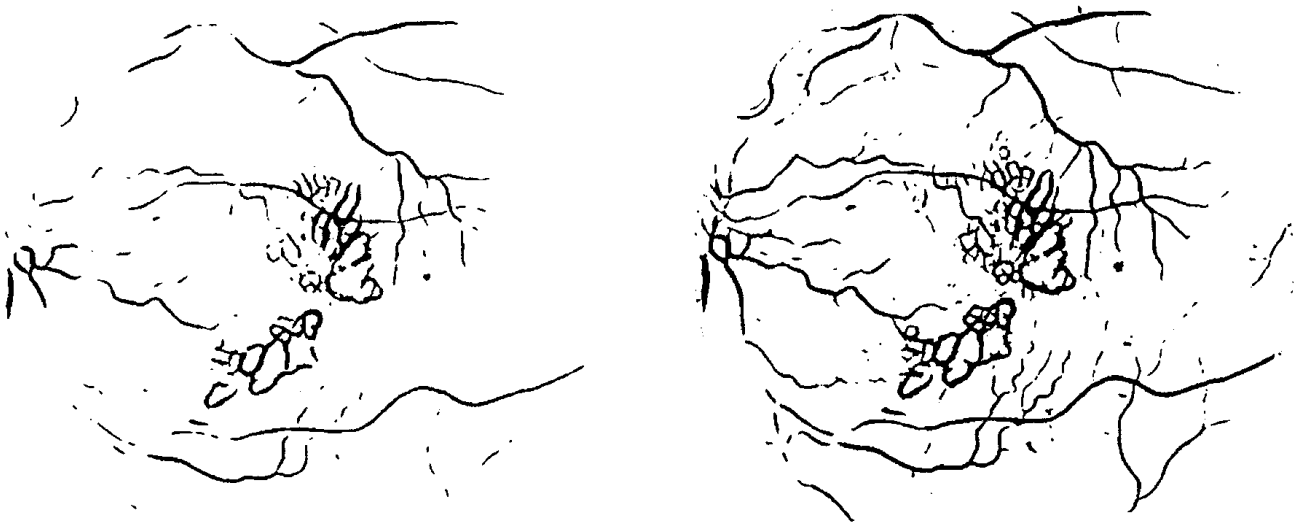


Fig. 2. (a) and (b) MFR thresholded at two different values. There is a strong overlap between true positive and false positive responses.

Used to detect pixels on the boundary of retinal vessels for subsequent grouping. In [16], a window surrounding a vessel pixel was modeled by a neural network trained on user selected examples. The drawback of these methods is that the large scale properties of vessels must be ignored to insure computational feasibility.

Classifier – based methods proceed in two steps. First a low level algorithm produces a segmentation of spatially connected regions. These candidate region are then classified as being vessel or not vessel. In [16], a window surrounding a vessel pixel was modeled by a neural network trained on user selected examples. the drawback of these methods is that the large scale properties of vessels(i.e. their network structure) must be ignored to insure computational feasibility.

Classifier – based method proceed in two steps. First a low level algorithm produces a segmentation of specially connected regions. These candidate region are then classified as being vessel or not vessel. In [21], regions segmented by user user – assisted thresholding were classified as blood vessel or leakage according to their length to width ratio. In [5], regions segmented by the method in [3] were classified as being vessel or not vessel. In [5], regions segmented by the method in [3] were classified as vessel or not vessel according to many properties, including their response to a classic operator designed to detect roads in aerial imagery[8]. The drawback of these these methods is that the large scale properties if vessel can not be applied to the problem until after the low level segmentation has already finished.

Therefore, these properties can not be used to drive the segmentation has already finished. Therefore, these properties cannot be used to drive the segmentation, merely to evaluate it.

Tracking based methods utilize a profile model to incrementally step along and segment a vessel. In [22], a Hough transform is used to locate the papilla in a retinal image. Vessel tracing proceeds iteratively from the papilla, halting when the response to a one – dimensional (1-D) (cross-section) matched filter falls below a given threshold. In [20], a similar method was employed to detect vessels in coronary arteriograms, from user given starting points. In [23], the tracking method was driven by a fuzzy model of a 1-D vessel profile. One drawback to these approaches is their proclivity for termination at branch points (whether real or caused by pathology), which are not detected well by 1-D filters. Another drawback is their reliance upon unsophisticated methods for locating starting points, which must always be either at the optic nerve or at subsequently detected branch points.

In [6], a method for tracking edge paths is used to segment arteries in cineangiograms. Edge paths are modeled as markov chains. A sequential edge linking (SEL) algorithm is introduced to search the possible set of paths for the best fit to the markov model. The probabilities of the model are adjusted to reflect the properties of the desired path, such as the tolerance to local curvature. A strength of this approach is that the grouping operation works upon actual gradient value, as opposed to a threshold response. Therefore, a segmentation decision is not reached until an arbitrary number of pixel is available for classification. A drawback to the approach is that branches are not modeled, so that each branch must be traced and classified independently.

In this work, we propose a new method for segmenting blood vessel in a retinal image. The MFR image, computed as described in [3], is thresholding using a novel probing technique. The probe examines the image in pieces, testing a number of region – based properties. If the probe decides a pieces is vessel, then the constituents pixels are simultaneously segmented and classified. Contrasted against classifier – based methods, our probing methods, allows a pixel to be tested in multiple region configuratio before final classification. Contrasted again tracking based methods, our probing method is driven by a two dimensional (2-D) MFR. Contrasted against [6], our probing method is region based and so naturally allows for multiple branches.

This paper expands upon a preliminary report given at the 1998 American Medical Informatics Association Annual Symposium [14].

III ALGORITHM

We first review the matched filter construction and convolution, described in [3], upon which our algorithm builds. We then present threshold probing and its application to blood vessel segmentation in a retinal image.

A. Matched filter for blood vessels

A matched filter describes the expected appearance of a desired signal, for purpose of comparative matching. In[3] a Gaussian function is proposed as a model for a blood vessel profile. The model is extended to two dimensions by assuming a vessel has a fixed width and direction for a short length. Since vessels may appear in any orientation, a set of 2-D segment profiles in equiangular rotations is used as a filter bank. The filters are implemented using twelve $16 * 16$ pixel kernels. The details for computing the actual values in the kernels may be found in [3].

The matched filter is applied by convolving a retinal image with all twelve kernels. The MFR is taken as the value for the highest scoring kernel at each pixel. On a Sun SPARCstation 20, the computation of the MFR image for a 700 605-pixel retinal image takes approximately 5 min. For purposes of threshold probing, the MFR image is normalized and quantized to eight bits per pixel.

B. Threshold probing

The basic operation of our algorithm is to probe regions in an MFR image. During each probe, a set of criteria is tested to determine the threshold of the probe, and ultimately to decide if the area being probed (termed a piece) is blood vessel. A flowchart for the algorithm is shown in figure.3. A queue of points is initialized, each of which will be used for a probe. Upon a probe's completion, if the piece is determined to be vessel, then the endpoints of the piece are added to the queue. In this way, different probes (and thus different thresholds) can be applied throughout the image.

The following steps initialize a queue of pixels which are to be used as starting points for probing.

- Convolve the matched filter described in[3] with the image, producing an MFR image.
- Using a histogram of the MFR image, threshold the image such that $>T_{\text{thresh}}$ pixels are above the threshold.
- Thin the thresholded image (for instance, using the algorithm given in [15,p.59]).
- In the thinned image, erase (relabel as background) all branch points, breaking up the entire foreground into segments that contain two endpoints each. Endpoints may be discovered as any pixel for which a traverse of the eight bordering pixels in clockwise order yields only one foreground transition. Similarly, branch points may be discovered as any pixel for which the same transverse yields more than two transitions.
- Discard segments with less than ten pixels.
- All remaining endpoints are placed in the probe queue.

The segments created by simple thresholding (above) are used only to locate a set of starting points to initialize the probe queue. The segments themselves will not appear in the final segmentation unless the probing procedure (below) cause their reappearance and classification as vessel. This process of initialization allows the pixels with a strong response to the matched filter to act as candidate vessels, with the design that not all need necessarily become part of the final vessel segmentation. Unlike tracking based methods[20],[22],[23], these starting points can be anywhere in the vessel network, so that pathology and branches do not cause parts of the network to be missed.

Each pixel in the probe queue is used as a starting point for threshold probing. The probing is iterative. The iterations are used to determine an appropriate threshold for the area being probed. The initial threshold is the MFR image value at the starting pixel. In each iteration, a region is grown from the start pixel, using a conditional paint-fill technique. The paint fill spreads across all connecting pixels that are not already labeled and that are above the current threshold. Once the paint-fill is complete, the desired attributes of the grown region are tested. If the region passes the tests, then the threshold is decreased by one and a new iteration begins. The technique is illustrated in fig.4.

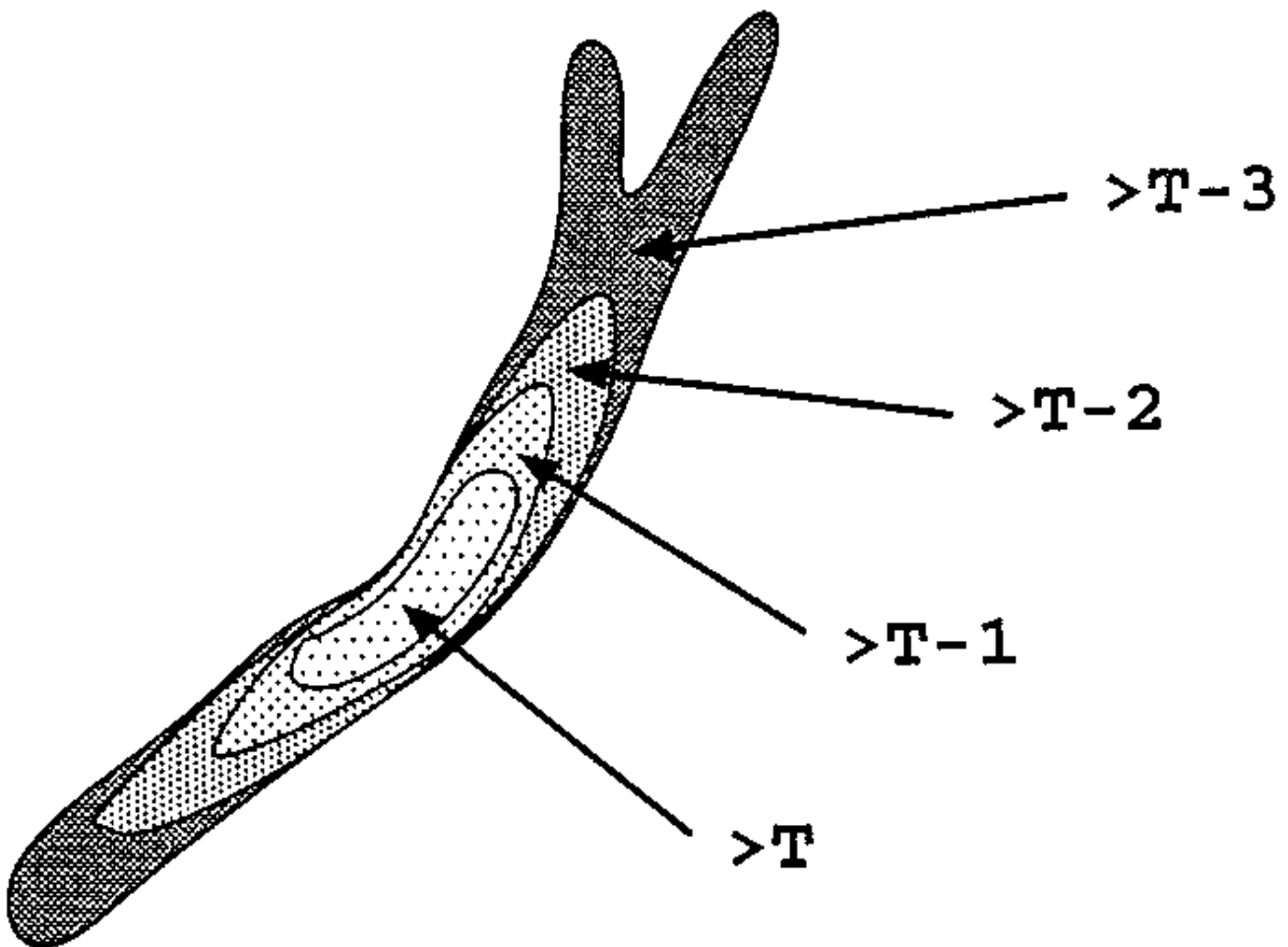


Fig. 4. The basis of threshold probing. At each iteration, a set of region tests is applied to determine if the threshold may be decreased an additional step. Local probing halts when any of the region tests fail.

Each probe iteration conducts the following tests.

- If the piece size (in pixels) exceeds T_{max} , then the probe halts. This requires multiple pieces (and thus potential multiple thresholds) to segment the entire image. The effect is that the probe adapts to the local strength of the MFR image.
- If the piece touches (on its border) more than one previously vessel-classified pieces, then the probe halts. This is particularly useful for bridging gaps along vessel exhibiting weak MFR values.
- If the ratio (border pixel touching another pieces / total pixels in piece) $> T_{fringe}$ then the piece is fringing, and the probe halts. This prevents a probe from searching along the borders of vessel pieces already segmented.

- If the ratio (total pixels – in- piece/ branch in piece) < Ttree, then the probe halts. This requires a piece to have a minimum span of vessel(s) per branch, and thus prevents over – branching down false paths. The count of branches in piece is found by calculating the skeleton of the piece at each iteration. The computational cost of this step is kept low by using indirect image indexing (a list of the image coordinates of the pixels in the piece.)

None of the tests relying upon thresholds (Tmax, Tfringe, Ttree) is performed until the piece reaches at least 30 pixels but less than Tmax pixels, or connects two previously probed pieces, then the region is labeled as vessel. The endpoints of the vessel piece are added to the queue. If the region is not determined to be vessel, then its pixels are left unlabeled. In either case, the next point in the queue is selected for probing. When the queue is empty, the algorithm is complete. Probes that begin at the endpoints of previously grown pieces have one additional constraint. An eight – pixel long artificial boundary is placed perpendicular to the end of the previously grown piece, to prevent the new pieces from probing back along the sides of the piece to probe in a new direction. These artificial boundaries are removed at the completion of the algorithm.

Some tests besides those listed above were explored during the development of this algorithm. Of particular note is a test for spatial looping, which is often caused by lesions and hemorrhages. Halting the probe when a loop is detected eliminates many of the false positive responses to these pathologies. However, it also halts probing wherever vessels cross each other at different depths of the retina. Without an explicit depth perception, these crossing appear exactly like loops. In the final analysis, these crossing appear exactly like loops. In the final analysis we abandoned the loop test because of this problem.

IV. IMAGES

Twenty retinal fundus slides were selected for testing the described method. The slides were captured by a TopCon TEV-50 fundus camera at 35° field of view. Each slide was digitized to produce a 605 * 700 pixel image, 24 bits per pixel (standard RGB). Ten of the images are of patients with no pathology (normals). Ten of the images contain pathology that obscures or confuses the blood vessel appearance in varying portions of the image (abnormals) . This selection was made for three reasons. First, most of the referenced methods have only been demonstrated upon normal vessel appearances, which are easier to discern. second, some level of success with nonnormal vessel appearance must be established to recommend clinical usage. Third, we desired to evaluate the performance difference (if any) of our algorithm no normal and abnormal cases.

Each of these 20 images was carefully labeled by hand, to produce a ground truth vessels segmentation. An example is shown in fig.5. the tool used for hand labeling is adapted from the tool described in [12], which was used to create hand – labeled images for evaluating range image segmentation algorithms. the tool allows the user to magnify the image to a level appropriate for labeling individual pixels, one at a time, as being vessel or not vessel. The tool also allows the user to apply various histogram transformations, to better visualize the original image data. The process of labeling an image takes several hours, depending on the user and image.

Fig 6 shows the distribution of MFR values for pixels hand labeled as vessel. Fig6(a) shows the distribution for the ten normal cases, fig(a) shows the distribution for the ten normal cases, fig 6(b) shows the distribution for the ten abnormal cases. Although there is a better separation between vessel and non vessel pixels In the normal cases. The results from Basic thresholding on an abnormal image , presented in fig.2 are explained by this overlap.

The classification of a majority of the pixel is often clear to a human observer. However, some of the pixels, such as those on the boundary of a vessel, those for small vessels, and those for vessel near pathology, are less easily labeled. To estimate this variance in observation, a second person produced an additional set of hand labeling for the 20 test images. For the results reported in section V, this second labeling is used to establish a reference for performance comparison.

On average , the first person labeled 32 200 pixels in each image as vessel, while the second person labeled 46 100 pixels in each image as vessel. Subsequent review indicate that the first person took a more conservative view of the boundaries of vessels and in the identification of small vessels than the second person. Both labelings for one of the normal images are shown in fig.7 we are making all the original retinal images and hand labelings available to any interested researchers for development and evaluation of related methods.

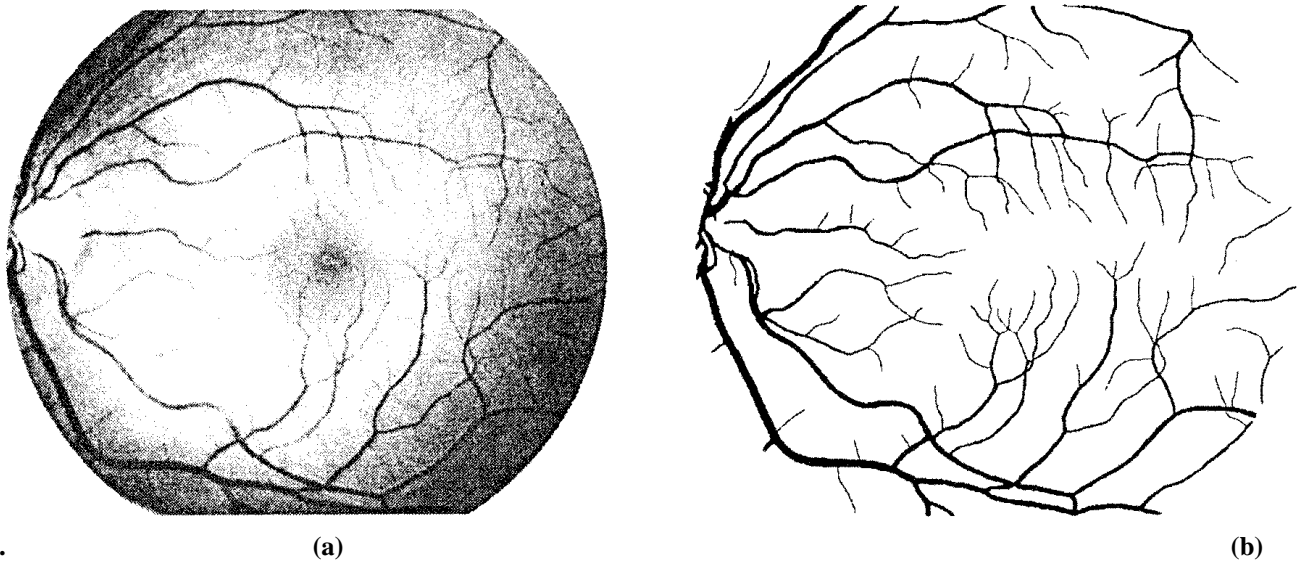


Fig. 5. (a) An example retinal image showing normal vessels. (b) A hand-labeled ground truth vessels segmentation.

V. EXPERIMENTS

The MFR images for all 20 images were processed using basic thresholding. Performance was established as follows. Any pixel which was hand labeled as vessel, whose MFR is also above the given threshold was counted as a true positive. Any pixel which was hand labeled as not vessel whose MFR is also above the given threshold was counted as false positive the true positive rate is established by dividing the number of true positive by the total count of pixels hand labeled as vessel. The false positive rate is established by dividing the number of false positive by the total count of pixels hand labeled as not vessel. Fig.8 shows the true positive and false positive detection rates across the range of possible thresholds.

Note that the false positive detection rate is considerably worse the abnormal cases than for the normal cases. By comparing the second hand -labeled images to the first hand – labeled images (using the same method as outlined for thresholding, above) we can establish a target performance level. This level is indicated by three isolated marks in fig. 8, showing the second person's performance on the normal, abnormal and average case. Note that the grouping of these three marks shows a small distribution, indicating that people may in fact be somewhat affected by the presence of pathology.

The shapes of the curve in Fig.8 are explained by reexamining the distribution of pixels shown in fig.6 the abnormal not only have a greater overlap, but also a biomedical distribution is caused by strong responses of the MFR to the boundaries of lesion , hemorrhages, and other pathology. This causes the dent in the abnormal's curve. Note also that the actual number of non-vessel pixels outnumbers the number of vessel pixels by a factor of ten. The appearance of a substantial number of false negatives occurs at a much higher threshold for the abnormal than for the normal (see fig.6), so that the average performance curve for a short range.

There are five parameters for our algorithm : T_{thresh} ; T_{min} ; T_{max} ; T_{fringe} . we report results processing all 20 of our images using ten sets of value for these parameters

Where each value of I represents one tested set of values. An example result processed at values in the middle of these sets is shown in fig. 9. Several functions similar to (1) were explored, by varying the initial vales and increments. This strategy was taken in lieu of a full five – parameter search for the best performance curve , which is computationally prohibitive. All 20 images were used to select the best parameters curve. However the additional parameter curve explored produced very similar results. Based on this observation we believe that the overestimation of performance caused by the absence of separate train and test sets is minimal in this case.

The performance curves for our algorithm on the normals, abnormal, and all images are shown in fig.10. for reference, the average performance mark for the second set of labeled images is included , as is the average performance curve for basic thresholding. Note that there is virtually no difference in the performance of our algorithm on normal or aabnormals. Also note that the performance of our algorithm reduces the number of false positive by as much as 15 times over basic thresholding of an MFR, at up to a 75% true positive rate. For these experiments, our algorithm appears to have a breaking point at an approximately 80% true positive rate. Our algorithm produces the same number of false positives ata 75% true positive rate as the second set of hand labeled images produces at a 90% true positive rate. This suggests room for an improvements of 15% in the true positive rate over our method.

III. SURVEY OF PROPOSED SYSTEM

This paper offers a prototype gadget of assistive textual content reading. The system framework includes three functional additives: scene capture, statistics processing, and audio output. The scene capture component collects scenes containing gadgets of interest in the form of pix or video. In our prototype, it corresponds to a camera connected to a couple of sunglasses. The facts processing thing is used for deploying our proposed algorithms, which includes 1) item-of-interest detection to selectively extract the image of the item held via the blind consumer from the cluttered historical past or different neutral gadgets in the digital camera view; and a couple of) text localization to reap picture areas containing text, and text popularity to convert picture-based totally text statistics into readable codes. We use a mini pc as the processing tool in our modern-day prototype machine.

The audio output component is to inform the blind consumer of identified textual content codes. A Bluetooth earpiece with mini microphone is employed for speech output. This simple hardware configuration guarantees the portability of the assistive text analyzing machine. Fig. four depicts a piece flowchart of the prototype gadget. A body collection V is captured via a digital camera worn by using blind customers, containing their handheld items and cluttered history.

VI. METHDOLOGY

1. OBJECT REGION DETECTION

To ensure that the hand-held object appears in the camera view, we employ a camera with a reasonably wide angle in our prototype system (since the blind user may not aim accurately). However, this may result in some other extraneous but perhaps text-like objects appearing in the camera view for example, when a user is shopping at a supermarket).

To extract the hand-held object of interest from other objects in the camera view, we ask users to shake the hand-held objects containing the text they wish to identify and then employ a motion-based method to localize the objects from cluttered background. Background subtraction (BGS) is a conventional and effective approach to detect moving objects for video surveillance systems with stationary cameras.

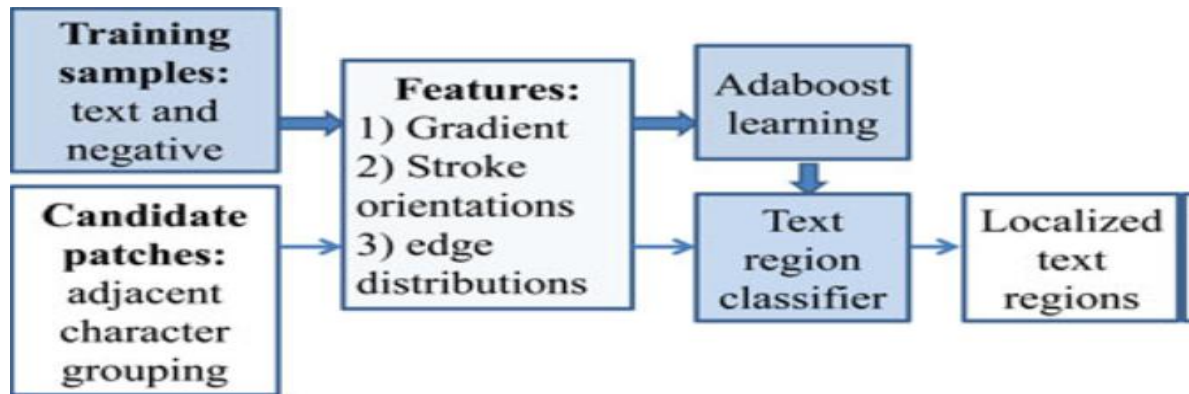


Fig. Diagram of the proposed Adaboost-learning-based text region localization Algorithm by using stroke orientations and edge distributions.

To detect moving objects in a dynamic scene, many adaptive BGS technique have been developed. Stauffer and Grimson modeled each pixel as a mixture of Gaussians and used an approximation to update the model. A mixture of K Gaussians is applied for BGS, where K is from 3 to 5. In this process, the prior weights of K Gaussians are online adjusted based on frame variations. Since background imagery is nearly constant in all frames, a Gaussian always compatible with its subsequent frame pixel distribution is more likely to be the background model.

2. AUTOMATIC TEXT EXTRACTION

We design a learning-based algorithm for automatic localization of text regions in image. In order to handle complex backgrounds, we propose two novel feature maps to extracts text features based on stroke orientations and edge distributions, respectively. Here, stroke is defined as a uniform region with bounded width and significant extent. These feature maps are combined to build an Adabost based text classifier

Text Stroke Orientation

Text characters consist of strokes with constant or variable orientation as the basic structure. Here, we propose a new type of feature, stroke orientation, to describe the local structure of text characters. From the pixel-level analysis, stroke orientation is perpendicular to the gradient orientations at pixels of stroke boundaries. To model the text structure by

stroke orientations, we propose a new operator to map a gradient feature of strokes to each pixel. It extends the local structure of a stroke boundary into its neighborhood by gradient of orientations. We use it to develop a feature map to analyze global structures of text characters.

3. TEXT RECOGNITION AND AUDIO OUTPUT

Text recognition is performed by off-the-shelf OCR prior to output of informative words from the localized text regions. A text region labels the minimum rectangular area for the accommodation of characters inside it, so the border of the text region contacts the edge boundary of the text character. However, our experiments show that OCR generates better performance if text regions are first assigned proper margin areas and binarized to segment text characters from background.

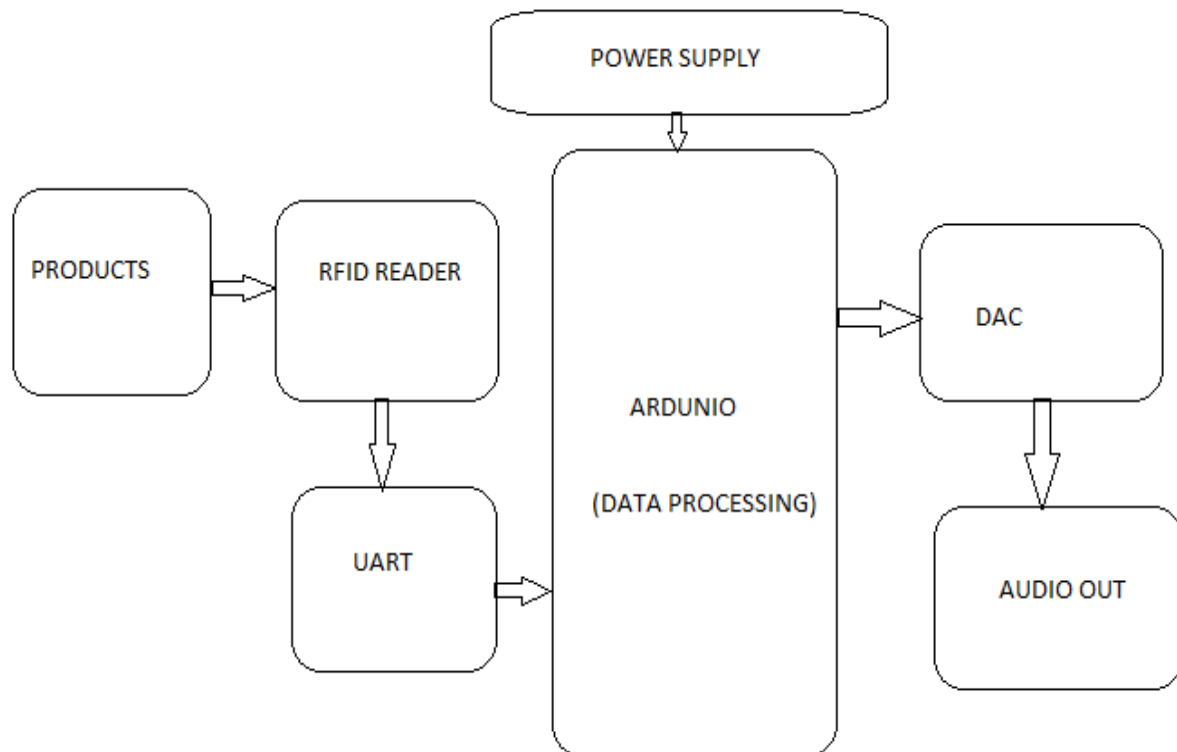
Thus, each localized text region is enlarged by enhancing the height and width by 10 pixels, respectively, and then, we use Otsu's method to perform binarization of text regions, where margin areas are always considered as background. We test both open- and closed-source solutions that allow the final stage of conversion to letter codes (e.g. OmniPage, Tesseract, ABBYReader).

Datasets

Two datasets are used to evaluate our algorithm. First, the ICDAR Robust Reading Dataset is used to evaluate the proposed text localization algorithm. The ICDAR-2003 dataset contains 509 natural scene images in total. Most images contain indoor or outdoor text signage. The image resolutions range from 640×480 to 1600×1200 .

Since layout analysis based on adjacent character grouping can only handle text strings with three or more character members, we omit the images containing only ground truth text regions of less than three text characters. Thus, 488 images are selected from this dataset as testing images to evaluate our localization algorithm.

IV. SYSTEM ARCHITECTURE



V. CONCLUSION

We've described a prototype device to examine published textual content handy-held objects for assisting blind men and women so one can remedy the common aiming problem for blind users, we've got proposed a motion-primarily based method to come across the item of interest, even as the blind user actually shakes the item for multiple seconds. This method can correctly distinguish the object of interest from historical past or other items inside the camera view. To extract text regions from complicated backgrounds, we've proposed a unique text localization set of rules based totally on

fashions of stroke orientation and facet distributions. The corresponding function maps estimate the worldwide structural function of text at each pixel. Block patterns mission the proposed feature maps of a photograph patch right into a feature vector. Adjacent man or woman grouping is performed to calculate applicants of textual content patches prepared for text classification. An advert enhance getting to know version is employed to localize text in digital camera-based totally photographs. Off-the-shelf OCR is used to carry out phrase recognition on the localized textual content areas and transform into audio output for blind customers. Our destiny work will extend our localization set of rules to system text strings with characters fewer than 3 and to layout more strong block patterns for text characteristic extraction. we are able to also enlarge our algorithm to deal with non-horizontal textual content strings. Moreover, we are able to deal with the extensive human interface troubles associated with studying textual content by using blind users

VI. REFERENCES

- [1] "10 facts about blindness and visual impairment", World Health Organization: Blindness and visual impairment, 2009. www.who.int/features/factfiles/blindness/blindness_facts/en/index.html
- [2] Advance Data Reports from the National Health Interview Survey, 2008. http://www.cdc.gov/nchs/nhis/nhis_ad.htm.
- [3] International Workshop on Camera-Based Document Analysis and Recognition (CBDAR 2005, 2007, 2009, 2011). <http://www.m.cs.osakafu-u.ac.jp/cbdar2011/>
- [4] X. Chen and A. L. Yuille, "Detecting and reading text in natural scenes," In *CVPR*, Vol. 2, pp. II-366 – II-373, 2004.
- [5] X. Chen, J. Yang, J. Zhang and A. Waibel, "Automatic detection and recognition of signs from natural scenes," In *IEEE Transactions on image processing*, Vol. 13, No. 1, pp. 87-99, 2004.
- [6] D. Dakopoulos and N. G. Bourbakis, "Wearable obstacle avoidance electronic travel aids for blind: a survey," In *IEEE Transactions on systems, man, and cybernetics*, Vol. 40, No. 1, pp. 25-35, 2010.
- [7] B. Epshtein, E. Ofek and Y. Wexler, "Detecting text in natural scenes with stroke width transform," In *CVPR*, pp. 2963-2970, 2010.
- [8] Y. Freund and R. Schapire, "Experiments with a new boosting algorithm," In *Int. Conf. on Machine Learning*, pp.148–156, 1996.
- [9] N. Giudice and G. Legge, Blind navigation and the role of technology, in *The engineering handbook of smart technology for aging, disability, and IEEE/ASME Transactions on Mechatronics* 10
- [10] X. Yang, S. Yuan, and Y. Tian, Recognizing Clothes Patterns for Blind People by Confidence Margin based Feature Combination, In *ACM Multimedia*, pp. 1097-1100, 2011.
- [10] A. Huete, J. Victores, S. Martinez, A. Gimenez, and C. Balaguer. Personal Autonomy Rehabilitation in Home Environment by a Portable Assistive Robot. In *IEEE Trans. Systems, Man, and Cybernetics, Part C: Applications and Reviews*, Vol. 42, No. 4, pp. 561-570, 2011.
- [11] ICDAR 2011 Robust Reading Competition: A. Shahab, F. Shafait, and A. Dengel. ICDAR Robust Reading Competition Challenge 2: Reading Text in Scene Images. In *Proceedings of ICDAR*, pp. 1491-1496, 2011.
- [12] K. Kim, K. Jung, and J. Kim, "Texture-based approach for text detection in images using SVM and continuously adaptive mean shift algorithm," In *IEEE Trans. on PAMI*, Vol.25, No.12, pp.1631-1639, 2003.
- [13] "KReader Mobile User Guide", knfb Reading Technology Inc, <http://www.knfbReading.com>
- [14] S. Kumar, R. Gupta, N. Khann